Bounded Step Superdiffusion in an Oriented Hexagonal Phase

Yann Gambin,[1] Gladys Massiera,[2,*] Laurence Ramos,[2] Christian Ligoure,[2] and Wladimir Urbach[1]

[1]*Laboratoire de Physique Statistique de l'Ecole Normale Superieure, UMR CNRS 8550, 24 rue Lhomond, 75005 Paris, France*
[2]*Laboratoire des Colloïdes Verres, et Nanomatériaux, UMR CNRS 5587, place Bataillon, 34095 Montpellier, France*

(Received 22 October 2004; published 22 March 2005)

Fluorescence recovery after pattern photobleaching is used to measure the self-diffusion of surfactant molecules, along cylinders and perpendicular to their main axis in an oriented hexagonal lyotropic phase. Unexpectedly, while the motion along cylinders is diffusive, a superdiffusive behavior is observed in the direction perpendicular to the cylinder axis. Moreover, varying the lattice parameter, we found that the perpendicular diffusion time is governed only by the number of cylinders to cross, providing experimental evidence for superdiffusion with a bounded step length.

DOI: 10.1103/PhysRevLett.94.110602 PACS numbers: 05.40.-a, 02.50.-r, 61.30.St, 82.70.-y

Increasing theoretical and experimental interest has turned towards the mechanisms leading to anomalous diffusion, i.e., sub- or superdiffusive behavior [1–3]. Subdiffusion for instance can arise from the presence of traps with long time release [4,5]. Superdiffusive behavior has been demonstrated in turbulent velocity fields [6,7]. On the other hand, when long range correlation or large scale transport do not exist, one can explain enhanced diffusion by the properties of the media, which create long steps with anomalous probability for the particle motion. If the step length distribution is broad, in such a way that its variance is infinite, the application of the central limit theorem fails and the statistics is not Gaussian anymore. Lévy flights correspond to a distribution of step length with a power law tail and give the preponderant role to rare events: as time goes on, the probe will undergo longer and longer steps; as the full sum is dominated by its largest terms, the apparent mobility is continuously increasing. While anomalous diffusion has been extensively studied theoretically and by numerical simulations [3,8,9], experimental examples of superdiffusion involving a Lévy flightlike process are scarce [10,11]. The first experimental evidence was provided by a system of polymerlike micelles [10], characterized by a broad distribution of size of breaking and recombining micelles.

In this Letter, fluorescence recovery after pattern photobleaching (FRAPP) is used to study the self-diffusion of fluorescent surfactant probes in oriented hexagonal phases of cylindrical micelles. The originality of our study is twofold: while in previous works [12] the motion of the probes has been assumed to be diffusive, FRAPP provides us with a tool to test the validity of these hypotheses. Unexpectedly, while the motion of the probes is diffusive along the cylinders, superdiffusion is systematically observed in the perpendicular direction, the distance covered by the probe increasing as $\tau^{1/2\mu}$, with $\mu < 1$. Furthermore, we are able to tune both the interfringe distance i of the pattern photobleaching and the lattice parameter of the hexagonal phase, λ, allowing one to independently change the q wave vector ($q = 2\pi/i$) and the number of cylinders per interfringe. We thus obtain master curves showing that the diffusion time perpendicular to the cylinders axis depends uniquely on the number of cylinders to cross.

Our experimental results are discussed in the framework of Lévy flights theory with fixed step length λ [13], which uses continuous time random walks formalism [14].

The hexagonal phases are composed of a mixture of sodium dodecylsulfate (SDS) as surfactant and pentanol as cosurfactant, brine, and cyclohexane. The cylinders are parallel to each other and form a periodic pattern of characteristic length λ in the direction perpendicular to their main axis (Fig. 1). By varying concomitantly the oil content and the ionic strength of the polar medium, the radius R of the oil-swollen cylinders is tuned between 55 and 150 Å, while the distance between them is kept nearly constant ($a \approx 25$ Å). The structure of this system has been extensively characterized elsewhere [15]. For the purpose of comparison, we also use a lamellar phase whose composition is close to that of the hexagonal phases. Fluorescent probes consisting of hydrocarbon tails of, respectively, 12 (C_{12}) and 18 (C_{18}) carbon groups, grafted to a fluorescein head are added at a concentration of about 10^{-5} M. Samples are prepared at 20 °C and introduced by suction into 200 μm thick flat microchannels, leading thus to oriented hexagonal phases with cylinders parallel to the long axis of the microcontainer [16]. The orientation of the

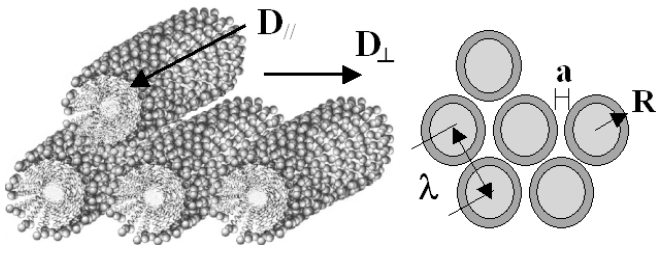

FIG. 1. Cartoon of the oriented hexagonal phase of surfactant cylinders. $D_{\parallel}$ and $D_{\perp}$ define the probe diffusion, respectively, in the directions parallel and perpendicular to the cylinder axis.

hexagonal phase is controlled between each experiment. An area of the sample is considered suitable if under a polarized microscope it appears completely black between crossed polarizers (when one of the polarizers is parallel to the main orientation of the cylinders), and if the area neighboring that spot is free of textures and defects. Samples are extremely stable, and any phase transition is easily detectable, betrayed by its well-known defect features.

The FRAPP technique is described in detail in Ref. [17]. Shortly, when illuminated by a high intensity laser flash (200 mW), the fluorescent molecules are irreversibly bleached. The recovery of fluorescence intensity $I(t)$ in the bleached areas is governed by the self-diffusion of the unbleached probes and monitored by a low intensity laser beam. In order to improve the signal-to-noise ratio, we use a fringe pattern, created by two laser beams intersecting exactly in the focal plane of a light microscope. Using various converging lenses, any fringe of size i between 1 and 150 μm can be obtained in a spot of diameter ranging from 50 μm up to 2 mm. The ability to observe the bleaching spot with the microscope allows a precise measure of the fringe size and a careful choice of the studied area. A goniometer ensures an accurate measurement of the angle of the cylinders with respect to the fringes. The fringe position is modulated at a frequency ω, and the signal is detected at ω and 2ω using a lock-in amplifier. In all experiments, monoexponential recoveries of fluorescence are measured: the signal at 2ω is proportional to $I_0[1 - \exp(-t/\tau)]$. The coefficient of diffusion D, in a privileged direction defined by the fringe pattern wave vector $\mathbf{q}$ ($q = 2\pi/i$), is deduced from $D = (\tau q^2)^{-1}$. For Brownian diffusion, D is q independent.

In the first set of experiments, the scattering vector $\mathbf{q}$ is fixed, and the sample rotates on a goniometer. The zero angle is defined as the angle θ, at which the sample is perfectly black between crossed polarizers. Figure 2 shows the angular dependence of the diffusion coefficient; D increases monotonically when θ varies between 0° and 90°. A fit with the simple equation

$$D(\theta) = D_\perp \cos^2(\theta) + D_\parallel \sin^2(\theta) \quad (1)$$

[18] describes perfectly the experimental data (inset of Fig. 2) and allows one to extract the diffusion coefficient along the micelles ($D_\parallel$) and perpendicular to their main axis ($D_\perp$). Furthermore, Fig. 2 demonstrates the high quality of the orientation on the bleaching spot length scale, as well as our ability to measure reliably the two diffusion coefficients, $D_\parallel$ and $D_\perp$. We find that the diffusion is highly anisotropic with $10^2 < D_\parallel/D_\perp < 10^3$.

We performed experiments on parallel and perpendicular mobilities, varying both the radius of the micelles and the hydrophobicity of the probes. Results for $D_\parallel$ are summarized in Fig. 3. For fringe size ranging from 5 to 150 μm, all samples exhibit Brownian diffusion as proved by the linear variation of τ^{-1} with q^2 (a typical plot is shown in the inset of Fig. 3). For both C_{12} and C_{18} probes, a similar increase of $D_\parallel$ is observed when the curvature of the surface over which the probe molecules diffuse is varied (from 0 for the lamellar phase down to $1/55$ Å^{-1} for the hexagonal phase with the smallest cylinders). Figure 3 shows that when the radius of the micelles decreases, the probe encounters a slightly increasing hindrance to its mobility, possibly due to steric interactions between the probe and SDS surfactant molecules. In addition, we find that, for a given curvature, $D_\parallel$ depends only slightly on the probe but is smaller for the C_{18} probe. In good agreement with the prediction of Cohen and Turnbull [19], and with previous experimental results [20] describing a diffusion governed by local defects in a surfactant layer, $D_\parallel$ is inversely proportional to the square root of the probe weight.

Strikingly, for all samples and all probes, an enhanced diffusion is observed in the direction perpendicular to the cylinders. We find that the distance covered by the probes

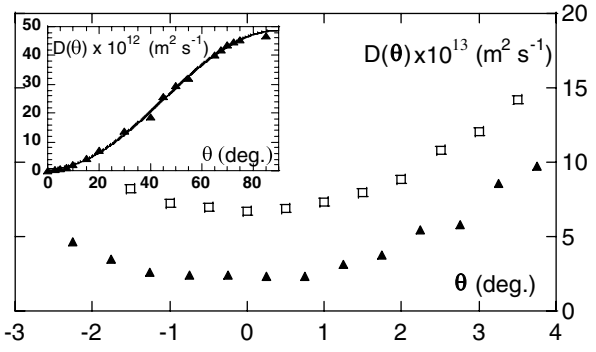

FIG. 2. Diffusion coefficient as a function of the angle between the $\mathbf{q}$ vector and the micelles long axis, for a sample with $R = 55$ Å. Main curve: Blowup around $\theta = 0$ with an interfringe $i = 6.6$ μm for (□) C_{12} and (▲) C_{18} probes. Inset: Full $D(\theta)$ curve for C_{18} and $i = 44$ μm. Solid line: Fit to the data [Eq. (1)] that yields $D_\parallel = 50 \times 10^{-12}$ m^2/s and $D_\perp = 0.7 \times 10^{-12}$ m^2/s.

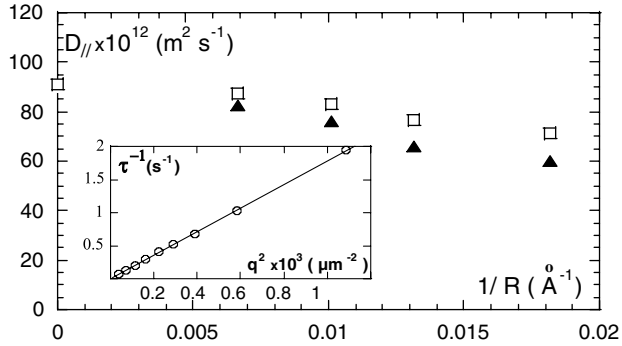

FIG. 3. Diffusion coefficient along the cylinders, $D_\parallel$, as a function of the inverse of the cylinder radius, for (□) C_{12} and (▲) C_{18}. Each point is obtained from the slope of a τ^{-1} vs q^2 plot (inset). Experimental errors are smaller than symbol size.

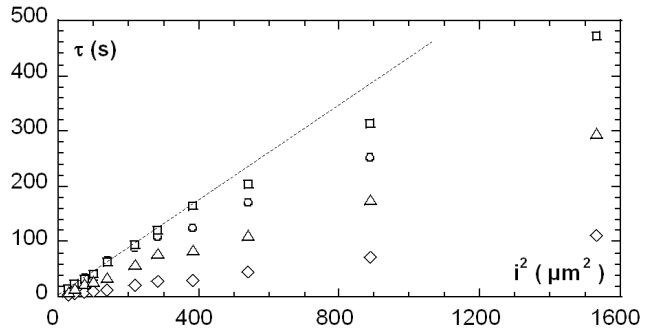

FIG. 4. Characteristic diffusion time τ of the C_{12} probe vs the square of fringe size i^2 for micelles of radius $R = 55$ (□), 76(○), 99(△), and 150 Å(◇). The dotted line represents a Brownian diffusion for $R = 55$ Å.

scales as $\tau^{1/2\mu}$, with exponents 2μ varying from 1.57 to 1.76. Figure 4 shows the diffusion time measured when the **q** vector is perpendicular to the cylinders as a function of the amplitude of the fringe size for C_{12} and for various cylinders radii. It was systematically found that τ decreases when R increases. However, if we rescale the interfringe by the lattice parameter of the hexagonal phase and plot the data as a function of $N = i/\lambda$, N being the number of cylinders encountered by the probes when traveling over a distance of an interfringe i, all the data gather onto a master curve (Fig. 5). Figure 6 proves that for both probes, over three decades of time, the master curves scale as a power law, $\tau = N^{2\mu}$, with $2\mu = 1.75 \pm 0.05$ for C_{12} and $2\mu = 1.65 \pm 0.05$ for C_{18}. The master curves demonstrate that the elementary step for diffusion is the lattice parameter. In other words, if the interfringe contains the same number of micelles, the characteristic relaxation time will be the same whatever the interfringe value is.

Before any further analysis of the enhanced diffusion, we note that we have carefully checked for possible artifacts in our measurement system. As the defects in orientation remain the same over days, and since no signal at ω has been observed by the lock-in amplifier, convection in our sample is excluded [17]. A careful choice of perfectly oriented areas allows one to determine the characteristic

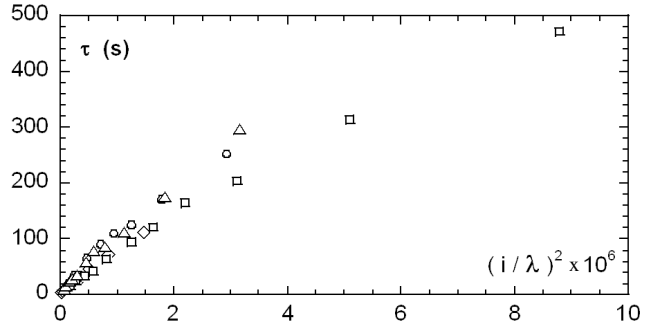

FIG. 5. Characteristic time τ versus the number of micelles crossed $(i/\lambda)^2$ for C_{12}: all the points from Fig. 4 (same symbols used) gather onto a master curve.

monoexponential recovery time τ with a precision better than 2%. From 15 °C up to 45 °C, we explored the limits of existence of the hexagonal phase without significant changes in the results. We have varied both the depth of the capillary from 100 to 200 μm and its width from 1 to 4 mm, as well as the concentration of fluorescent molecules and the intensity of the laser beam, without influencing on the results. We have checked that a pattern with a 10 μm interfringe created inside bleaching spots of 50, 100, 200, 500 μm up to 2 mm (width of the microchannel) takes precisely the same time to relax.

The three main results obtained for the self-diffusion in the direction perpendicular to the cylinders show that (i) the diffusion is controlled by the ratio between the interfringe and the lattice parameter, (ii) the motion of the probe is superdiffusive, and (iii) different probes have a slightly different behavior, depending on their affinity for the micellar core. Unlike the classic Lévy flights, the diffusion $D_\perp$ can be seen as a random walk with a fixed step length equal to the lattice parameter λ, as suggested by the master curve (Fig. 5). The diffusion is indeed self-similar; i.e., the time needed for a probe to travel on a distance equal to the fringe size does not depend on that specific size nor on the cylinder radius, but on the number of cylinders to cross. In a lattice of cylindrical micelles which are intuitively expected rather to act as "traps," superdiffusion seems paradoxical. However, it could stem from a purely statistical mechanism [13]. The basis of the model is to consider no longer the waiting time distribution but the number of steps undergone by the probe in a fixed interval of time, the step length being fixed. If a strong fluctuation of step density exists in the system, and if the first moment of the density diverges, the mean residence time will vanish and the number of events can grow superlinearly with time. As time runs, the probe will undergo longer and longer series of quick steps in a self-similar manner, eventually leading to the observed enhanced diffusion. Such extreme events can be very rare; the key to

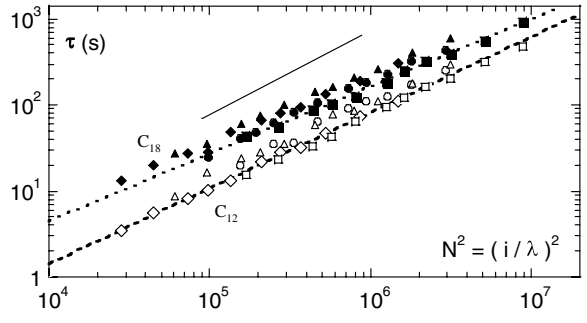

FIG. 6. Characteristic time τ versus the number of micelles crossed N $(= i/\lambda)$ by C_{12} (solid symbols) and C_{18} (open symbols) probes. Dotted lines are the best fits obtained with a power law $\tau = N^{2\mu}$, with $2\mu = 1.75 \pm 0.05$ for C_{12} and 1.65 ± 0.05 for C_{18}. For comparison, the slope $\tau = N^2$ is represented by the solid line.

anomalous diffusion is given by the enormous number of events occurring during the interval of time considered. From the fact that two distinct master curves are obtained for C_{12} and C_{18} (Fig. 6), we can infer that the step density depends on the hydrophobic tail of the probe and that the more hydrophobic the probe, the longer is its residence time within a micelle. More quantitatively, we find that, for a given N, the ratio between the characteristic times measured with the two probes, $\tau_{C_{18}}/\tau_{C_{12}}$, ranges between 2 and 4. Nevertheless, the differences in τ are smaller than one would expect according to Boltzmann coefficients [$\exp(6)$ by taking $1k_BT$ per carbon group] for a complete extraction of the probe from the micelle.

Among the various hypotheses, a mechanism of diffusion based on breaking and recombining micelles carrying the probe should be eliminated since, as in Ref. [10], one would measure the mobility of the micelle itself, and the results would be independent of the probe tail length (C_{12} or C_{18}). The presence of static defects allowing the probe to cross one or several micelles would result in a diffusive behavior as shown for dislocations in a lamellar phase [21,22]. The microscopic mechanism leading to superdiffusion in our system could find its origin in the probe tail conformation. In the case when, from time to time, the hydrophobic tail is not fully inserted into the hydrophobic core of the micelle, the probe will likely leave its micelle earlier than expected. Another mechanism that could affect the step density would be collisions between cylinders allowing probes to be transferred from one cylinder to the other with a probability which would depend on the bending modulus of the cylinder. In either case, if the process repeats itself for a certain number of steps, one could obtain a significant acceleration of the probe. Both mechanisms could possibly occur simultaneously.

In conclusion, we show that the diffusion of surfactant molecules is indeed anisotropic and that their motion in the direction perpendicular to the cylinders is superdiffusive and self-similar, i.e., governed by the number of cylinders to cross rather than the distance to travel. The microscopic origin of this superdiffusive behavior remains to be clarified, but the above described system is, to our knowledge, the first experimental evidence for superdiffusion with a bounded step length.

We thank C. Blanc for fruitful discussions.

*Present Address: Laboratoire de Spectrométrie Physique, BP 87, 140 avenue de la Physique, 38402 St. Martin d'Hères, France.

[1] I. M. Sokolov, J. Klafter, and A. Blumen, Phys. Rev. E **64**, 021107 (2001).
[2] R. Metzler and J. Klafter, Phys. Rev. E **61**, 6308 (2000).
[3] M. F. Shlesinger and G. M. Zaslavsky, in *Levy Flights and Related Topics in Physics*, edited by Uriel Frisch (Springer, New York, 1994).
[4] J. P. Bouchaud and E. M. Bertin, Phys. Rev. E **67**, 026128 (2003).
[5] I. Y. Wong *et al.*, Phys. Rev. Lett. **92**, 178101 (2004).
[6] J. P. Bouchaud *et al.*, Phys. Rev. Lett. **64**, 2503 (1990).
[7] A. R. Osborne and R. Caponio, Phys. Rev. Lett. **64**, 1733 (1990).
[8] D. Brockmann and T. Geisel, Phys. Rev. Lett. **90**, 170601 (2003).
[9] I. M. Sokolov, J. Mai, and A. Blumen, Phys. Rev. Lett. **79**, 857 (1997).
[10] A. Ott *et al.*, Phys. Rev. Lett. **65**, 2201 (1990).
[11] T. H. Solomon, E. R. Weeks, and H. L. Swinney, Phys. Rev. Lett. **71**, 3975 (1993).
[12] D. Constantin *et al.*, J. Phys. Chem. B **105**, 668 (2001); D. Constantin and P. Oswald, Phys. Rev. Lett. **85**, 4297 (2000).
[13] I. M. Sokolov, Phys. Rev. E **63**, 011104 (2001).
[14] H. Scher and E. W. Montroll, Phys. Rev. B **12**, 2455 (1975).
[15] L. Ramos and P. Fabre, Langmuir **13**, 682 (1997).
[16] M. Impéror-Clerc and P. Davidson, Eur. Phys. J. B **9**, 93 (1999).
[17] R. Messager *et al.*, Phys. Rev. Lett. **60**, 1410 (1988); J. Davoust, P. F. Devaux, and L. Léger, EMBO J. **1**, 1233 (1982).
[18] M. W. Hamersky *et al.*, Macromolecules **31**, 5363 (1998).
[19] M. H. Cohen and D. Turnbull, J. Chem. Phys. **31**, 1164 (1959).
[20] A. Maldonado, W. Urbach, and D. Langevin, J. Phys. Chem. B **101**, 8069 (1997).
[21] R. L. Blumberg Selinger, Phys. Rev. E **65**, 051702 (2002).
[22] V. Gurarie and A. E. Lobkovsky, Phys. Rev. Lett. **88**, 178301 (2002); D. Constantin and R. Holyst, Phys. Rev. Lett. **91**, 039801 (2003).